

See discussions, stats, and author profiles for this publication at: <https://www.researchgate.net/publication/281909811>

Determination of Kinetic Parameters within a Single Nonisothermal On-Flow Experiment by Nanoliter NMR Spectroscopy

ARTICLE in ANALYTICAL CHEMISTRY · SEPTEMBER 2015

Impact Factor: 5.64 · DOI: 10.1021/acs.analchem.5b02811

READS

36

7 AUTHORS, INCLUDING:



Antonio M Rodriguez Garcia

University of Naples Federico II

21 PUBLICATIONS 76 CITATIONS

SEE PROFILE



Antonio de la Hoz

University of Castilla-La Mancha

270 PUBLICATIONS 3,712 CITATIONS

SEE PROFILE



Raluca M Fratila

University of Zaragoza

43 PUBLICATIONS 354 CITATIONS

SEE PROFILE

Determination of Kinetic Parameters within a Single Nonisothermal On-Flow Experiment by Nanoliter NMR Spectroscopy

M. Victoria Gomez,^{*,†,∇} Antonio M. Rodriguez,^{†,∇} Antonio de la Hoz,[†] Francisco Jimenez-Marquez,[‡] Raluca M. Fratila,^{§,||} Peter A. Barneveld,[⊥] and Aldrik H. Velders^{*,†,#}

[†]Instituto Regional de Investigación Científica Aplicada, Campus Universitario, Avenida Camilo José Cela s/n, 13071 Ciudad Real, Spain

[‡]Escuela Técnica Superior de Ingenieros (ETSI) Industriales, Universidad de Castilla-La Mancha, Avenida Camilo José Cela s/n, 13071 Ciudad Real, Spain

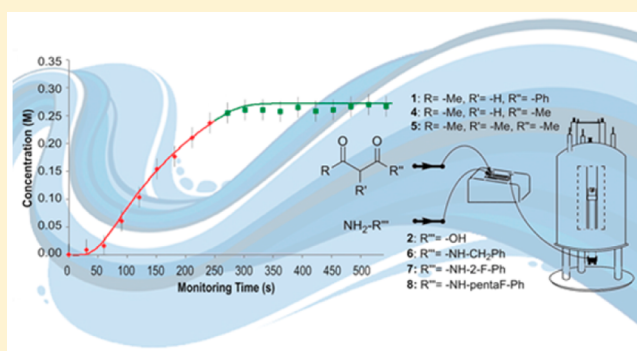
[§]Instituto de Nanociencia de Aragón (INA), Universidad de Zaragoza, C/Mariano Esquillor s/n, 50018 Zaragoza, Spain

^{||}Fundación Agencia Aragonesa para la Investigación y Desarrollo (ARAID), C/María de Luna 11, 50018 Zaragoza, Spain

[⊥]Laboratory of Physical Chemistry & Soft Matter and [#]Laboratory of BioNanoTechnology, Wageningen University, Dreijenplein 6, 6703 HB Wageningen, The Netherlands

Supporting Information

ABSTRACT: Conventional methods to determine the kinetic parameters for a certain reaction require multiple, separate isothermal experiments, resulting in time- and material-consuming processes. Here, an approach to determine the kinetic information within a single nonisothermal on-flow experiment is presented, consuming less than 10 μmol of reagents and having a total measuring time of typically 10 min. This approach makes use of a microfluidic NMR chip hyphenated to a continuous-flow microreactor and is based on the capabilities of the NMR chip to analyze subnanomole quantities of material in the 25 nL detection volume. Importantly, useful data are acquired from the microreactor platform in specific isothermal and nonisothermal frames. A model fitting the experimental data enables rapid determination of kinetic parameters, as demonstrated for a library of isoxazole and pyrazole derivatives.



Determination of kinetic parameters for a reaction, i.e., activation energy and pre-exponential factor, usually requires measuring the initial reaction rate for different initial substrate concentrations, at various (constant) temperatures, and fitting the data to the corresponding reaction rate law, resulting in a time- and material-consuming process.¹ Here, we report a procedure utilizing a continuous-flow microreactor hyphenated to a microfluidic NMR chip, enabling the rapid determination of the kinetic parameters within a single on-flow experiment consuming only micromole quantities of reagents.

Microreactors constitute a revolutionary alternative for a wide range of chemical applications. The advantages of microreactor technology regarding process control conditions, uniform temperature distribution, and efficient mixing by virtue of a short diffusion path, stemming from its small size and high surface-to-volume ratio, also make it ideal for the extraction of reaction kinetic information.^{2–5} To take full benefit of working on-flow, for process control of reactions, for reaction kinetics studies, and for quality specifications and overall system performance,^{6,7} the online integration of detection techniques is required. Fluorescence,⁸ ultraviolet–visible absorption,⁹

infrared,¹⁰ Raman,¹¹ X-ray,¹² and NMR¹³ spectroscopy as well as time-resolved ESI-MS¹⁴ are being explored as online/in-line or in situ instrumentation integrated with microreactors. Recently, different methodologies have been developed involving in-line/online analytical techniques (i.e., HPLC, Raman, and IR) coupled to microreactors which are focused on the generation of kinetic data, by allowing the microreactor to reach the steady state of the reaction.^{2,15,16} Raman spectroscopy provided fast acquisition of location-specific information about the reaction profile along a microreactor channel,^{2,4} while in-line IR spectroscopy allows for a rapid generation of time-series reaction data by manipulating the flow rate and reaction temperature.¹⁵

NMR is widely applicable in industrial and technical environments where a “noninvasive” analytical technique is desirable. Most importantly, NMR provides both qualitative and quantitative information from a reaction, and can operate

Received: July 25, 2015

Accepted: September 18, 2015

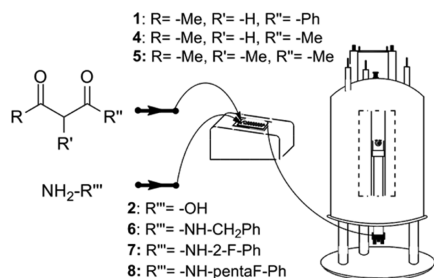


under process conditions without any need for a calibration effort,^{17,18} also in in-line mode hyphenating conventional reaction vessels with tailor-made tubings.^{19,20} When working with small amounts of material, e.g., in microreactors, the intrinsically low sensitivity of NMR can be overcome with implementation of small transceiver coils, as the signal-to-noise ratio increases with a decrease in the coil diameter.^{21–24} We have reported novel microfluidic chip designs for the monitoring of supramolecular interactions at the picomole level by ¹⁹F NMR,²⁵ as well as multinuclear 1D and 2D NMR experiments with a single nonresonant microcoil.²⁶

In a previous paper,²⁷ we reported the use of a microfluidic NMR chip hyphenated to a continuous-flow microliter microwave irradiation system for online monitoring and rapid optimization of reaction conditions. The active volume of the NMR chip was chosen much smaller with respect to that of the microwave flow cell to allow the analysis of different zones of the reaction volume separately. Considering the very short onset of the microwave (time needed to attain the maximum heating power and target temperature, e.g., 2 s for 125 °C and about 5 s for 150 °C), switching on the irradiation power when working under flow conditions results in portions of the reaction volume being exposed to microwave irradiation for different times. Consequently, multiple data points could be sampled (conversion vs reaction time) from a single on-flow experiment, virtually subdividing the microwave reaction volume (1.6 μL) in portions that one after the other reach the NMR chip (detection volume 6 nL). Three independent experiments were performed at three different constant temperatures, yielding the typical exponential growth or decay curves as expected for isothermal measurements of the product or reagents, respectively, against residence/reaction time.^{15,2}

Here, we report a new procedure to rapidly extract kinetic information from a chemical reaction, by means of a hyphenated microreactor platform–NMR microfluidic chip setup (Scheme 1). This procedure is based on the capabilities

Scheme 1. Schematics of the Labtrix Start–NMR Hyphenated Setup^a



^aThe reaction zone consists of a 20 μL microreactor, connected by means of capillaries to a microfluidic NMR chip fixed inside the bore of a superconducting 9.4 T NMR magnet. Compounds 2, 7, and 8 were used as HCl salts.

of the NMR chip of analyzing very small portions of the reaction volume from the microreactor platform (Labtrix Start) before, at the onset of, and during the steady state of the reaction; the data can be fit against a reaction conversion model. This approach allows the extraction of the reaction order, rate constant, and Arrhenius parameters within a single nonisothermal on-flow experiment by remote analysis of different (2.5 μL) volume fractions of the 20 μL microreactor.

We proof the operational efficacy of this method with monitoring the preparation of a small library of isoxazole ring and pyrazole derivatives.

EXPERIMENTAL SECTION

General Procedures. NMR spectra for characterization and identification of (new) compounds were recorded on a Varian Inova 500 MHz spectrometer in CD₃OD at 298 K and at 499.769 and 125.678 MHz for ¹H and ¹³C NMR, respectively. Chemical shifts were referenced to the solvent peak (CD₃OD, 3.31 ppm). Assignment of the spectra was carried out using g-COSY, g-HMQC, g-HMBC, TOCSY, NOESY, and ¹³C NMR experiments (¹⁹F-decoupled and ¹H-decoupled). Two-dimensional NMR spectra were acquired typically using 96 scans and 128 increments. The pulse programs were taken from the standard Varian pulse sequence library. All spectra were Fourier transformed with MestReNova 8.1 software. High-resolution mass spectrometry (HRMS) was carried out with a chromatography/electron ionization mass spectrometry (EI-MS) system (GCT, Waters). Commercially available starting materials and solvents were used without previous purification.

Reaction Conversion Model. We assume the microreactor to heat up according to Newton's law of heating, leading to the following heating characteristic:

$$T = T_f - (T_f - T_i) \exp(-\tau t) \quad (1)$$

Here, T_i and T_f are the initial and final temperatures, respectively, and t is the so-called monitoring time, viz., the time elapsed after heating was switched on. The proportionality factor τ was calculated experimentally by measuring the dependency of the Labtrix heating plate temperature on time (see Figure S1). This temperature dependency was used to solve the second-order rate laws

$$\frac{d[A]}{dt} = -k(T)[A]^2 \quad (2)$$

and

$$\frac{d[P]}{dt} = -\frac{d[A]}{dt} \quad (3)$$

where $[A]$ is the reactant concentration and $[P]$ the product concentration. For the temperature dependency of the second-order rate constant k the well-known Arrhenius equation was applied:

$$k(T) = A \exp(-E_a/RT) \quad (4)$$

with A being the pre-exponential factor and E_a the activation energy of the reaction. Note that according to eq 1 the temperature T is time dependent.

For the sake of clarity, it is convenient to consider two consecutive cohorts of 20 μL (the microreactor volume), each subdivided into eight sample volumes of 2.5 μL. With the maximum residence time in the chip of a sample fraction defined as t_R , then the first cohort consists of sample volumes spanning from monitoring time zero to t_R and the second cohort spans from t_R to $2t_R$. Maple 16 software was used to solve the differential equations numerically. The two cohorts were treated separately and differently. For the first cohort, the time spent in the microreactor is equal to the monitoring time t . It then suffices to solve the equations with initial values $[A] = [A]_0$ and $[P] = 0$ from $t = 0$ to t_R , and to use intermediate time

values as desired. The second cohort of sample fractions always spends t_R time in the microreactor, so for each data point, and for each point in the curve, a *separate* integration over the time interval t_R is to be conducted. The same initial concentrations are used as before, but this time the integration goes from $t - t_R$ to the actual monitoring time t , and the final value of the integration is used. Using this scheme to calculate the concentrations at any desired monitoring time t , the data points were fitted manually to the Arrhenius parameters A and E_a . Consecutively, the conversion was determined for a second-order reaction in time (for the first cohort of volume fractions) followed by a cohort with constant reaction time, yet variable temperatures for the different volume fractions.

Hyphenated Setup. A Labtrix Start microreactor, which is a commercial continuous-flow reactor defined to evaluate many reaction parameters in a short period of time, was hyphenated to a microfluidic NMR chip. When the Labtrix Start microreactor was placed inside the magnetic stray field of the spectrometer magnet, we recorded a difference of 6 deg between the temperature set and the real temperature, utilizing a Pt-100 probe as the temperature sensor. *Safety note! Take care when bringing equipment with magnetic components into the magnet's stray field. They might unexpectedly be attracted by the magnet. Particularly the nonshielded magnets have large stray fields.* The tubing of the Labtrix Start microreactor (length 30 cm, o.d. 787 μm , i.d. 125 μm) was connected to a microfluidic NMR chip through microfluidic connections (fused-silica capillaries, length 1.2 m, o.d. 365 μm , i.d. 100 μm). A microreactor of 20 μL was used. The microfluidic NMR chip was designed using Clewin Layout Editor (version 4.3.3.0) and fabricated as described before.²⁶ The dimensions of the microfluidic NMR chip define a volume underneath the microcoil of 25 nL (detection volume). The total volume of the system, from the syringes to the NMR coil, is 50 μL . An overall flow rate of 5 $\mu\text{L}/\text{min}$ was used to develop the methodology for isoxazole and pyrazole derivatives, corresponding to 4 min for the first volume portion to reach the NMR chip.

Methodology. Two syringes with the corresponding starting material dissolved in methanol were loaded into the hyphenated Labtrix Start–NMR system at a specific flow rate and a final concentration of starting material in the reaction mixture of 0.375 M. While on-flow, the reaction temperature was set to 393 K, and the final temperature was reached in 1.5 min. Consecutive ^1H NMR experiments were launched. The ^1H NMR acquisition parameters for an experiment with a flow rate of 5 $\mu\text{L}/\text{min}$ were as follows: 30 accumulated scans, 1 s acquisition time and 0.05 s delay time, resulting in an NMR experiment time of 30 s, and an accumulated volume detected per NMR experiment of 2.5 μL . The volume of the Labtrix microreactor was 20 μL , which with these experimental conditions was (virtually) subdivided into eight 2.5 μL zones that were analyzed separately.

Control experiments were performed as follows: the Labtrix Start–NMR hyphenated setup was left to reach steady state, waiting a time corresponding to the flow through of 3 times the reactor volume, and the data of the reagent conversion into product were collected for different residence times at a certain temperature (368, 382, 404, and 420 K).

1-(2-Fluorophenyl)-3,5-dimethylpyrazole (12). Two separated syringes with pentane-2,4-dione (4) (0.75 M) and (4-fluorophenyl)hydrazine hydrochloride (7) (0.75 M) in CH_3OH were connected with an overall flow rate of 5 $\mu\text{L}/$

min (96% conversion). Orange liquid. Bp: 81.7 °C. ^1H NMR (CD_3OD , ppm): 7.54–7.51 (1H, m, 4'-H), 7.52–7.48 (1H, m, 5'-H), 7.43 (1H, cd, $J = 7.7, 1.4$ Hz, 3'-H), 7.32 (1H, td, $J = 7.6, 1.5$ Hz, 6'-H), 6.11 (1H, s, 4-H), 2.18 (3H, s, 3- CH_3), 2.09 (3H, s, 5- CH_3). ^{13}C NMR (CD_3OD , ppm): 156.6 (2'-C, d, $^1J_{\text{C-F}} = 250.5$ Hz), 131.1 (4'-C, d, $^3J_{\text{C-F}} = 8.3$ Hz), 129.7 (5'-C, s), 126.8 (1'-C, d, $^2J_{\text{C-F}} = 12.0$ Hz), 125.6 (6'-C, d, $^3J_{\text{C-F}} = 3.6$ Hz), 117.0 (3'-C, d, $^2J_{\text{C-F}} = 20.5$ Hz), 149.37, 142.1 (4-C), 106.9 (4-C), 13.6 (3- CH_3), 11.4 (5- CH_3). ^{19}F NMR (CD_3OD , ppm): -124.2 to -124.3 (1F, m). HR-MS: $\text{C}_{11}\text{H}_{11}\text{N}_2\text{F}$, calcd 190.092, found 191.6944 ($M + 1$).

1-(2-Fluorophenyl)-3,4,5-trimethylpyrazole (13). Two separated syringes with 3-methylpentane-2,4-dione (5) (0.75 M) and (4-fluorophenyl)hydrazine hydrochloride (7) (0.75 M) in CH_3OH were placed into the microreactor platform at an overall flow rate of 5 $\mu\text{L}/\text{min}$ (95% reaction conversion). Colorless oil. ^1H NMR (CD_3OD , ppm): 7.60–7.50 (1H, m, 4'-H), 7.50–7.40 (1H, m, 5'-H), 7.44 (1H, td, $J = 8.0, 2.0$ Hz, 3'-H), 7.35 (1H, t, $J = 7.6$ Hz, 6'-H), 2.16 (3H, s, 3- CH_3), 2.03 (3H, s, 5- CH_3), 1.93 (3H, s, 4- CH_3). ^{13}C NMR (CD_3OD , ppm): 156.3 (1'-C, d, $^1J_{\text{C-F}} = 249.5$ Hz), 131.1 (4'-C, d, $^3J_{\text{C-F}} = 8.6$ Hz), 129.4 (5'-C, s), 126.1 (1'-C, d, $^2J_{\text{C-F}} = 11.9$ Hz), 125.3 (6'-C, d, $^3J_{\text{C-F}} = 4.0$ Hz), 116.7 (3'-C, d, $^2J_{\text{C-F}} = 18.6$ Hz), 147.4 (3-C), 138.9 (5-C), 112.7 (4-C), 11.3 (3- CH_3), 9.6 (5- CH_3), 7.74 (4- CH_3). ^{19}F NMR (CD_3OD , ppm): -124.2 to -124.3 (1F, m). HR-MS: $\text{C}_{12}\text{H}_{13}\text{N}_2\text{F}$, calcd 204.105, found 205.7243 ($M + 1$).

1-(2-Fluorophenyl)-5-methyl-3-phenylpyrazole (14). Two separated syringes with 1-phenylbutane-1,3-dione (1) (0.75 M) and (4-fluorophenyl)hydrazine hydrochloride (7) (0.75 M) in CH_3OH were placed into the microreactor platform at an overall flow rate of 5 $\mu\text{L}/\text{min}$ (99% reaction conversion). Orange oil. ^1H NMR (CD_3OD , ppm): 7.81–7.79 (2H, m, 2''-H, 6''-H), 7.60–7.58 (1H, m, 5'-H), 7.58–7.56 (1H, m, 4'-H), 7.41–7.39 (1H, m, 6'-H), 7.40–7.39 (2H, 3''-H, 5''-H), 7.39–7.38 (1H, m, 3'-H), 7.34–7.31 (1H, m, 4''-H), 6.66 (1H, s, 4-H), 2.24 (3H, s, 3- CH_3). ^{13}C NMR (CD_3OD , ppm): 158.7 (2'-C, d, $^1J_{\text{C-F}} = 250.0$ Hz), 154.1 (3-C), 144.3 (5-C), 134.3 (1''-C), 132.4 (4'-C, d, $^3J_{\text{C-F}} = 7$ Hz), 130.7 (5'-C), 129.8 (3''-C, 5''-C), 129.3 (4''-C), 128.5 (1'-C, d, $^2J_{\text{C-F}} = 13$ Hz), 126.9 (2''-C, 6''-C), 126.3 (6''-C, d, $^3J_{\text{C-F}} = 4$ Hz), 117.8 (3'-C, d, $^2J_{\text{C-F}} = 20$ Hz), 104.5 (4-C), 9.8 (CH_3). ^{19}F NMR (CD_3OD , ppm): -124.03 to -124.1 (1F, m). HR-MS: $\text{C}_{16}\text{H}_{13}\text{N}_2\text{F}$, calcd 252.105, found 253.3267 ($M + 1$).

1-(Pentafluorophenyl)-3,5-dimethylpyrazole (15). Two separated syringes with pentane-2,4-dione (4) (0.75 M) and (2,3,4,5,6-pentafluorophenyl)hydrazine hydrochloride (8) (0.75 M) in CH_3OH were placed into the microreactor platform at an overall flow rate of 5 $\mu\text{L}/\text{min}$ (96% reaction conversion). Brown liquid. Bp: 90.3 °C. ^1H NMR (CD_3OD , ppm): 6.18 (1H, s, 4-H), 2.26 (3H, s, 3- CH_3), 2.17 (3H, s, 5- CH_3). ^{13}C NMR (CD_3OD , ppm): 153.3 (3-C), 145.5 (2'-C, 6'-C, ddt, $^1J_{\text{C-F}} = 254.5$ Hz, $^2J_{\text{C-F}} = 13$ Hz, $^3J_{\text{C-F}} = 4$ Hz), 144.8 (5-C), 143.6 (4'-C, ddt, $^1J_{\text{C-F}} = 255$ Hz, $^2J_{\text{C-F}} = 14$ Hz, $^3J_{\text{C-F}} = 4$ Hz), 139.4 (3'-C, 5'-C, dddd, $^1J_{\text{C-F}} = 252.5$ Hz, $^2J_{\text{C-F}} = 13$ and 14 Hz, $^3J_{\text{C-F}} = 4$ Hz), 115.7 (1'-C), 107.9 (4-C), 13.4 (3- CH_3), 10.6 (5- CH_3). ^{19}F NMR (CD_3OD , ppm): -148.5 (2F, 3'-F, 5'-F, br d, $^3J_{\text{F-F}} = 16.5$ Hz), -154.9 (1F, 4'-F, tt, $^3J_{\text{F-F}} = 22.60$ Hz, $^4J_{\text{F-F}} = 3.7$ Hz), -164.1 (2F, 2'-F, 6'-F, td, $^3J_{\text{F-F}} = 19.0$ Hz, $^4J_{\text{F-F}} = 3.7$ Hz). HR-MS: $\text{C}_{11}\text{H}_7\text{N}_2\text{F}_5$, calcd 262.055, found 262.0522.

1-(Pentafluorophenyl)-3,4,5-trimethylpyrazole (16). Two separated syringes with 3-methylpentane-2,4-dione (5)

(0.75 M) and (2,3,4,5,6-pentafluorophenyl)hydrazine hydrochloride (**8**) (0.75 M) in CH₃OH were placed into the microreactor platform at an overall flow rate of 5 μ L/min (95% reaction conversion). Orange solid. Mp: 79.9–80.6 °C. ¹H NMR (CD₃OD, ppm): 2.22 (3H, s, 3-CH₃), 2.10 (3H, s, 5-CH₃), 2.01 (3H, s, 4-CH₃). ¹³C NMR (CD₃OD, ppm): 150.8 (3-C), 145.5 (2'-C, 6'-C, ddt, ¹J_{C-F} = 252.4 Hz, ²J_{C-F} = 12 Hz, ³J_{C-F} = 4 Hz), 143.4 (4'-C, ddt, ¹J_{C-F} = 255 Hz, ²J_{C-F} = 13 Hz, ³J_{C-F} = 4 Hz), 140.0 (5-C) 139.4 (3'-C, 5'-C, dddd, ¹J_{C-F} = 254 Hz, ²J_{C-F} = 12 and 13 Hz, ³J_{C-F} = 4.0 Hz), 116 (1'-C), 113.5 (C-4), 10.3 (3-CH₃), 7.7 (5-CH₃), 6.4 (4-CH₃). ¹⁹F NMR (CD₃OD, ppm): -148.7 (2F, 3'-F, 5'-F, br d, ³J_{F-F} = 17 Hz), -155.3 (1F, 4'-F, tt, ³J_{F-F} = 19.0 Hz, ⁴J_{F-F} = 2.8 Hz), -164.3 (2F, 2'-F, 6'-F, td, ³J_{F-F} = 18.8 Hz, ⁴J_{F-F} = 3.7 Hz). HR-MS: C₁₂H₉N₂F₅ calcd 276.07, found 276.0680.

1-(Pentafluorophenyl)-5-methyl-3-phenylpyrazole (17). Two separated syringes with 1-phenylbutane-1,3-dione (**1**) (0.75 M) and (2,3,4,5,6-pentafluorophenyl)hydrazine hydrochloride (**8**) (0.75 M) in CH₃OH were placed into the microreactor platform at an overall flow rate of 5 μ L/min (99% reaction conversion). Yellow oil. ¹H NMR (CD₃OD, ppm): 7.42 (1H, tt, *J* = 5.0, 1.0 Hz, 4''-H), 7.34–7.31 (2H, m, 3''-H, 5'-H), 7.25–7.22 (2H, m, 2''-H, 6''-H), 6.49 (1H, s, 4-H), 2.34 (3H, s, 3-CH₃). ¹³C NMR (CD₃OD, ppm): 152.3 (3-C), 147.6 (5-C), 145.2 (3'-C, 5'-C, ddc, ¹J_{C-F} = 254 Hz, ²J_{C-F} = 14 Hz, ³J_{C-F} = 4 Hz), 143.3 (4'-C, ddt, ¹J_{C-F} = 255 Hz, ²J_{C-F} = 13 Hz, ³J_{C-F} = 4 Hz), 139.1 (2'-C, 6'-C, dddd, ¹J_{C-F} = 252.5 Hz, ²J_{C-F} = 14 and 13 Hz, ³J_{C-F} = 4 Hz), 130.0 (3''-C, 5''-C), 129.7 (4''-C), 128.6 (2''-C, 6''-C), 126.6 (1''-C), 11.4 (3-CH₃). ¹⁹F NMR (CD₃OD, ppm): -147.6 (2F, 3'-F, 5'-F, br d, ³J_{F-F} = 18.0 Hz), -154.1 (1F, 4'-F, tt, ³J_{F-F} = 22.4 Hz, ⁴J_{F-F} = 3.7 Hz), -163.3 (2F, 2'-F, 6'-F, td, ³J_{F-F} = 19.3 Hz, ⁴J_{F-F} = 3.7 Hz). HR-MS: C₁₆H₉N₂F₅, calcd 324.068, found 324.8993.

RESULTS AND DISCUSSION

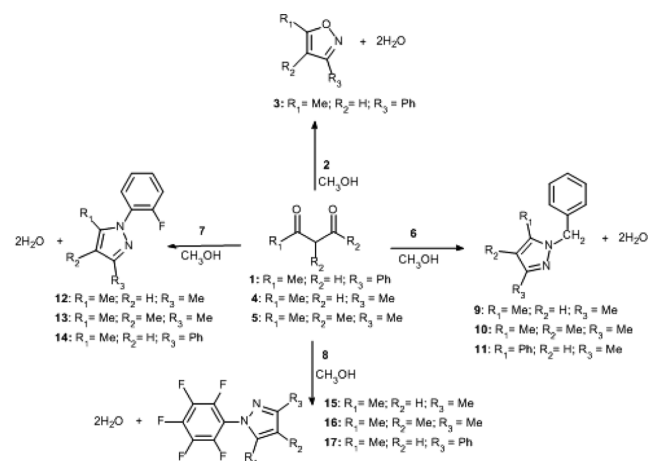
The hyphenated system consists of a commercial, continuous-flow microreactor (Labtrix Start) and a nanoliter NMR setup, comprising a 20 μ L reaction volume for the glass microreactor and a 25 nL NMR detection volume (Scheme 1). The detection volume of the NMR chip was chosen much smaller with respect to the microreactor volume to allow flexibility for monitoring of different reaction volumes and times, the flow rate, and/or correlated reaction conditions, adapting the acquisition parameters, e.g., number of scans, accordingly.

In general, a microreactor platform allows the reaction parameters to be evaluated in a short period of time, employing low amounts of material because of the small volumes of the chips (typically 20 μ L for the microreactor platform herein employed, a Labtrix Start system). This platform, similarly to other commercial or homemade microreactors, is nevertheless rather conventional in its standard operation mode, providing one data point per experiment at constant temperature and residence time. Moreover, the Labtrix Start reactor utilizes pulse width modulation control technology to provide accurate temperature control of thermoelectric devices; however, the temperature is not reached instantaneously, in contrast to the microwave reactor, previously employed in a hyphenated system with a nanoliter NMR microfluidic chip.²⁷ Because of this onset of the variable temperature (VT) unit of around 1.5 min, an equilibration time of 3 times the reactor volume is recommended by the manufacturer, before monitoring of the reaction itself is started. We believed the hyphenation of an

NMR chip to the Labtrix Start (or to any other microreactor where temperature is not reached instantaneously) could provide reaction parameters even faster than when using the Labtrix Start alone, monitoring during and, most interestingly, before the system reaches the steady-state temperature. As a consequence, the hyphenated setup allows the use of even much less material.

Reaction Scheme and Acquisition of Data. The reaction of 1-phenylbutane-1,3-dione (**1**) and hydroxylamine hydrochloride (**2**) for the synthesis of 5-methyl-3-phenylisoxazole (**3**) (Scheme 2)^{28–30} was chosen as a model reaction to illustrate

Scheme 2. Scheme for the Reaction in Methanol of 1-Phenylbutane-1,3-dione (1), Pentane-2,4-dione (4), and 3-Methylpentane-2,4-dione (5) with Hydroxylamine Hydrochloride (2), Benzylhydrazine Hydrochloride (6), (4-Fluorophenyl)hydrazine Hydrochloride (7), and (2,3,4,5,6-Pentafluorophenyl)hydrazine Hydrochloride (8)^a



^aThe analysis of the reaction mixture after some time does not show any reversibility.

the performance of the setup; to further illustrate the versatility of the developed methodology, the formation of a small library of pyrazole derivatives has also been investigated (Scheme 2).

Two syringes with the corresponding starting material dissolved in methanol were loaded into the Labtrix Start–NMR system at a 5 μ L/min overall flow rate and final starting material concentration of 0.375 M. [Note that a relatively high concentration of material (0.375 M) is required to achieve an appropriate signal to noise ratio (SNR) for the analysis. This is due to the small detection volume of the rf microcoil, i.e., 25 nL.] While on-flow, the reaction temperature was set to 393 K, and was reached in around 1.5 min. In-line, remote monitoring of the process resulted in a collection of NMR spectra showing the appearance and disappearance of reaction product and starting material, respectively, in time (Figure 1). Every NMR spectrum corresponds to a small volume fraction (e.g., 2.5 μ L) of the microreactor volume, recorded as the accumulated number of scans on-flow (i.e., 30).

Analysis of a Sigmoidal Curve. When the Labtrix Start reactor is hyphenated with a nanoliter NMR setup, the monitoring of the product concentration versus experiment time does not provide the typical exponential growth/decay curve for product/reagent, as expected for constant temperature measurements,^{1,27,2,15} rather a sigmoid-shaped curve is observed (Figure 2). The first data points differ from the typical

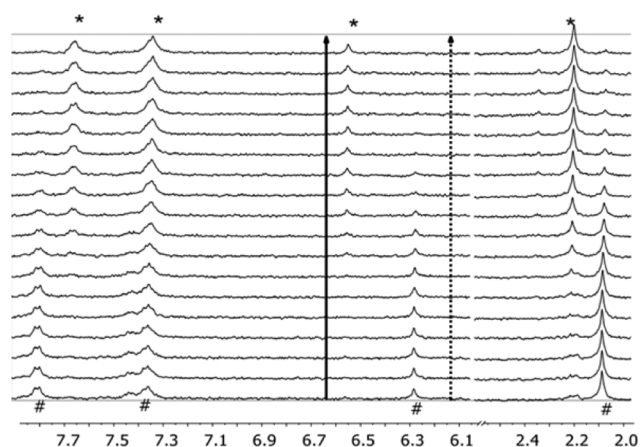


Figure 1. ^1H NMR spectra (ppm) for the synthesis of 5-methyl-3-phenylisoxazole (**3**). Each spectrum corresponds to a volume fraction of $2.5\ \mu\text{L}$ and an NMR experiment time of 30 s. The solid arrow is next to a peak that corresponds to the product; the dotted arrow is next to a peak of the reagent. The pound signs indicate reagent peaks (7.86, 7.49, 7.43, 6.32, and 2.12 ppm), and the asterisks indicate product peaks (7.72, 7.40, 6.58, and 2.26 ppm). The 6.0–2.7 ppm (solvent peaks) section was omitted for clarity.

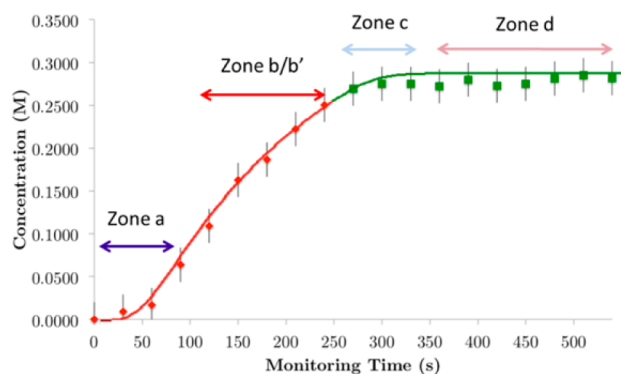


Figure 2. Reaction product concentration (M) versus monitoring time (s) for the synthesis of 5-methyl-3-phenylisoxazole (**3**) for an overall flow rate of $5\ \mu\text{L}/\text{min}$. Every data point corresponds to a $2.5\ \mu\text{L}$ fraction. The lowest product concentration data point corresponds to the detection of just 0.25 nmol of product in a 25 nL detection volume. The solid line has been obtained from fitting to a model. The red data points correspond to the first bunch of eight $2.5\ \mu\text{L}$ fractions, defined as zones a and b/b', which concern fractions with a variable residence time. The green data points correspond to the second bunch of fractions, defining zones c and d, of which all measured fractions have a constant residence time in the microreactor of 4 min.

exponential curve since they do not correspond to constant temperature measurements as the onset of the temperature unit takes around $1\frac{1}{2}$ min. Although this might seem inconvenient at first, it actually does allow for a rapid determination of the Arrhenius parameters without the need to do multiple temperature experiments, since extra information can be extracted within a single on-flow experiment. In fact, this feature was used for the determination of the reaction order, reaction rate constants, and Arrhenius parameters of the whole library of isoxazole and pyrazole derivatives as shown in Scheme 2.

When working at $5\ \mu\text{L}/\text{min}$, the flow-through time in a $20\ \mu\text{L}$ microreactor is 4 min. Optimizing the acquisition parameters in the ^1H NMR experiment (e.g., 30 accumulated

scans of 1 s at a flow rate of $5\ \mu\text{L}/\text{min}$ results in a detection volume per NMR experiment of $2.5\ \mu\text{L}$ with an NMR experiment time of 30 s) provides multiple data points that can be sampled, corresponding to different residence times. In other words, fractions of $2.5\ \mu\text{L}$ can be analyzed independently by means of the NMR microfluidic chip in a single nonisothermal on-flow experiment (Figure 2), each fraction corresponding to a different residence time or temperature profile experienced. [Note: The number of data points extracted from a microreactor volume is optimized in terms of an appropriate SNR for the analysis. Hence, this number (or the information regarding residence time) is restricted by the intrinsic features of the setup, i.e., sensibility and NMR detection volume. The type of chemical reaction also influences the amount of information that can be extracted within a single on-flow experiment.]

Except for the benzylhydrazine series, vide infra, the reactions chosen have a negligible conversion at room temperature (rt), and the reaction is considered to start once the sample is heated above rt and to stop when it exits the reactor. [Note: When benzylhydrazine hydrochloride (**6**) was used as the hydrazine derivative, it was necessary to quench the reaction at the point when it exited the microreactor. Hereto, acetone was used in a 1:10 acetone:reaction mixture ratio.] This fact is of high importance for the determination of the effective residence times at a given temperature. At the exit of the $20\ \mu\text{L}$ reactor volume, the reaction mixture enters the capillary that runs to the NMR chip. We carefully checked that the temperature dropped to rt when the reaction mixture exited the reactor chip. This was tested by measuring conversion while cooling or not cooling the capillary at the reactor outlet point, as well as by quenching the reactions by adding acetone at the end of the reactor through the in-built additional channel inlet. For the experiment, the Labtrix heating is switched on when the system is already on-flow; this defines time zero. To appreciate the different zones which can be distinguished by the remote NMR measurements (because of the slow temperature onset), two consecutive microreactor volumes can be discriminated, each of which has eight virtual sampling points of $2.5\ \mu\text{L}$ fractions (Figure 3). For clarity sake, we will refer to the “first cohort of eight fractions” when talking about the first microreactor volume and the “second cohort” for the second microreactor volume. Both of these sets of eight data points have some points corresponding to constant temperature or nonconstant temperature. Similarly, some data points have a constant time or a nonconstant residence time. Finally, some have a “starting concentration” at “time zero”, A_0 , of 0.375 M (a, b, c, d) or $<0.375\ \text{M}$ (b').

The first reactor volume is emptied from the chip starting at time zero, and this cohort of eight sample volumes have an incremental residence time going from 1 to 4 min, similar to the above-described microwave–NMR setup.²⁷ However, an important difference is the fact that the heating of the microreactor is not instantaneous, but takes 1.5 min before the set temperature is reached (Table S1 and Figure S1). Hence, two different sets of points can be differentiated within the first cohort leaving the microreactor, i.e., before and after temperature stabilization (zones a and b/b', respectively, Figure 3) (red data points, Figure 2). Every data point in zones a and b, detected on-flow as a $2.5\ \mu\text{L}$ portion in the NMR chip, has experienced a different residence time, from 1 to 4 min. Importantly, rather than defining each volume fraction to a unique combination of residence and temperature profile

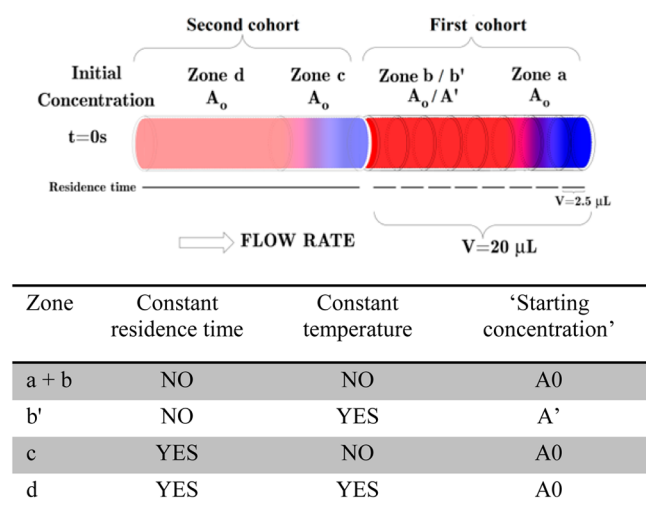


Figure 3. (Top) Schematics of two microreactor cohorts of sample fractions. Collections of data points are grouped in different zones (a, b/b', c, d). These zones differ from each other in temperature experienced once they exit the chip (red color representing volume fractions that have experienced the constant and final temperature for a certain amount of time at the moment they exit the chip, purple representing the ones that have not reached the final temperature (a) or have experienced a temperature gradient before exiting the chip (c)). Zone b fractions have experienced a temperature gradient but consecutively a constant temperature, and hence can also be treated as a classical isothermal experiment (b'). Residence times go from 0 to t_R in zones a and b/b' (discontinuous line, eight different portions can be analyzed) or are constant, t_R (continuous line). (Bottom) Table with differences among the zones (a + b, b', c, d) in residence time, temperature, and concentration.

experienced, a subset of data points, i.e., b', can be distinguished for zone b as volume fractions that have experienced the same constant temperature value for different residence times in the monitoring time frame of 90–240 s. In fact, the data points in zone b' can be identified with a typical exponential kinetic curve where the concentration of product is determined after various time intervals (for a certain initial concentration of reactants) and at a constant temperature, in contrast to zone a where the temperature is not constant yet (Figures 2 and 3). The data points in zone b' reflect a conventional kinetics experiment with a standard isothermal reaction conversion profile. Importantly, the “starting concentration” of the starting material to be taken into account in the analysis and calculations for zone b', vide infra, is lower than the initial concentration of starting material of 0.375 M, as a result of all volume fractions having been exposed to temperatures between room temperature and the final temperature for the first 90 s of the monitoring time “that define the zone a conditions”.

Regarding the second cohort of fractions that is monitored in the NMR chip, a third set of points (zone c) and a fourth set of points (zone d) can be discriminated (Figure 2, green data points). All these volume fractions of the second cohort have been in the microreactor for the maximum residence time t_R of 4 min, but they differ in experienced temperature profile: (similar to zone a) zone c volume fractions entered the microreactor before temperature stabilization (Figure 3), while the following fractions (zone d) entered the microreactor when the temperature was stable. Therefore, the different zones (a, b, c, and d) differ in temperature, residence time, and remarkably

the “effective starting concentration of reactants” (Figures 2 and 3).

Determination of the Reaction Order and Arrhenius Parameters. The reaction between 1-phenylbutane-1,3-dione (1) and hydroxylamine hydrochloride (2) (Scheme 2) can be expected to follow a second-order rate law, and as the concentration of both reagents is identical, the first eight (time-dependent) data points shown in Figure 2 are plotted as $1/[A]$ versus time (Figure 4). In fact, data points 4–8 define a

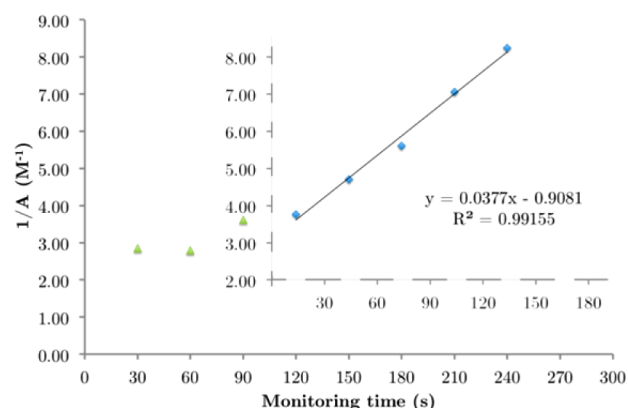


Figure 4. Inverse of reagent concentration ($[A]$) versus residence/monitoring time for the synthesis of 5-methyl-3-phenylisoxazole (3) for a flow rate of 5 $\mu\text{L}/\text{min}$. Note that only data points from the first cohort of fractions measured are shown (zones a and b/b'). Hence, the monitoring time equals the residence time of a fraction in the microreactor. The inserted dashed x- and y-axes emphasize the zone b' data points, which represent a “conventional” data set with incremental residence time and a constant temperature.

straight line corresponding to the isothermal points of zone b', corroborating the second-order rate law of this type of reaction. [Note: The data points that define a straight line indicate experimentally the moment when the microreactor platform reaches the steady state (constant temperature) and also the duration of the steady state.] From the slope, the reaction rate constant, k , is determined, and an intercept with the $1/[A]$ y-axis gives the initial concentration at the point of temperature stabilization within the microreactor volume. Note that the intercept is not the y-axis intercept of the extrapolated straight line at monitoring time zero, but the intercept of the virtually shifted y-axis at a time of 2 min. A reaction rate constant value of $0.038 \text{ M}^{-1} \text{ s}^{-1}$ and $[A]_0$ value of 0.277 M are extracted ($y = 0.0377x - 0.9081$). The latter data indicate that 0.24 μmol per volume fraction (2.4 nanomol per 25 nL NMR detection volume) was consumed in the microreactor at the point of reaching constant temperature, i.e., the starting point of zone b'. The overall reaction order is usually established by studying a reaction using different initial concentrations of reagents.¹ Focused on corroborating the reaction order in our studies, the initial concentrations of 1-phenylbutane-1,3-dione (1) and hydroxylamine hydrochloride (2) were reduced to half. Observing a decrease of 4-fold in the reaction rate confirms this to be a second-order reaction.

In a conventional approach, once the reaction order and rate constant have been determined, the reaction is studied over a range of temperatures as wide as possible, extracting the reaction rate constant from a conversion vs reaction time series at each temperature. Finally, the activation energy and the frequency factor are estimated when the reaction rate constants

at different temperature values are fitted to the Arrhenius equation.¹ The intrinsic features of the hyphenated Labtrix Start–nanoliter NMR microfluidic chip setup bring an advantage in the acquisition and treatment of kinetics data. The multiple NMR data points extracted, within a single on-flow experiment, provide direct information on the reaction kinetics at different temperatures and different “starting” concentrations. Note that the methodology developed here has not been tested for reactions that exhibit different rate laws for different temperatures.

For example, looking into zone a (three points), every data point corresponds to a different temperature (Table S1). Similarly, zone b' shows five data points with a constant temperature value (but different from those of zone a). Zone c includes the first three data points which entered the microreactor before temperature stabilization, each with a different temperature value, and zone d includes the following data points which experienced the constant temperature of 393 K for 4 min (but importantly, with a difference in “starting” concentration from that of zone b'). When all this experimental information, about different temperatures, temperature gradients, starting concentrations, and residence times obtained from a single on-flow experiment, are fitted within a theoretical model (Maple software; see the Experimental Section), it is possible to extract the Arrhenius parameters, pre-exponential factor, and activation energy values in a rapid manner from one single flow experiment.

When the data points shown in Figure 2 are fitted to the theoretical model, the following values are obtained: $A = 3.7 \times 10^9 \pm 1.85 \times 10^8 \text{ M}^{-1} \text{ s}^{-1}$ and activation energy of $79.1 \pm 3.0 \text{ kJ/mol}$ ($18.9 \pm 0.72 \text{ kcal/mol}$) (Table 1). Values for the pre-

Table 1. Arrhenius Parameters Extracted from the Experimental Data and Fitting Model for the Formation of Compounds 3, 9, 10, 11, 12, 13, 14, 15, 16, and 17

product	reaction rate constant ($\text{M}^{-1} \text{ s}^{-1}$)	pre-exponential factor ($\text{M}^{-1} \text{ s}^{-1}$)	activation energy (kJ/mol)
3	0.038	3.7×10^9	79.1
9	0.137	2.00×10^9	75.7
10	0.193	4.00×10^9	75.9
11	0.113	6.00×10^8	73.4
12	0.129	1.85×10^9	75.4
13	0.130	4.00×10^9	75.8
14	1.511	9.00×10^9	76.9
15	0.134	1.00×10^9	73.3
16	0.168	6.00×10^8	75.8
17	0.310	1.00×10^8	76.7

exponential factor, $A = 4.0 \times 10^9 \pm 1.2 \times 10^8$, and for the activation energy of $82.8 \pm 2.5 \text{ kJ/mol}$ ($19.8 \pm 0.6 \text{ kcal/mol}$) were obtained in a control experiment when the Labtrix Start–NMR hyphenated setup operated under steady-state conditions and the conventional approach¹ for the extraction of kinetic information was carried out (see Table S2 and Figure S2). This result validates the methodology developed herein.

When the Labtrix Start hyphenated setup works under steady-state conditions to carry out the “conventional” isothermal control experiment, 6 h is needed for extracting the kinetic information, in contrast to the 30 min (triplicating data for error estimation) needed when the information is extracted using the methodology reported here.

Preparation of a Library of Derivatives. Focused on illustrating the validity of this approach, the application of the methodology presented above was extended to a series of diketone and hydrazine derivatives in the formation of differently substituted pyrazole rings, thus extracting the corresponding kinetic information from these reactions. 1-Benzylhydrazine (6), (4-fluorophenyl)hydrazine hydrochloride (7), and (2,3,4,5,6-pentafluorophenyl)hydrazine hydrochloride (8) were combined with 1-phenylbutane-1,3-dione (1), pentane-2,4-dione (4), and 3-methylpentane-2,4-dione (5) (Scheme 1). This sums up nine pyrazole derivatives (9–17) of the previously prepared isoxazole ring; six of them (12, 13, 14, 15, 16, 17) are not previously described in the literature, defining a small library of heterocyclic rings.

The experimental conditions employed (393 K, $t = 4 \text{ min}$) were suitable to reach very high conversion for all cases using a $5 \mu\text{L/min}$ flow rate. The experiments were completed after 500 s. Thus, when pentane-2,4-dione (3) was employed, 96% conversion of reagent in the final product was observed for all hydrazine derivatives. Similarly, the use of 3-methylpentane-2,4-dione (4) afforded 95% conversion, and 1-phenylbutane-1,3-dione (1) afforded 99% maximum conversion for all cases.

Regarding the use of 1-benzylhydrazine (6), Figures S3 and S4 show the product concentration versus experiment time and $1/[A]$ versus experiment time, respectively, for the formation of 1-benzyl-3,5-dimethylpyrazole^{31–33} (9). Figure S5 and S6 correspond to 1-benzyl-3,4,5-trimethylpyrazole³³ (10). Figures S7 and S8 represent the experimental data obtained for 1-benzyl-5-phenyl-3-methylpyrazole (11).^{34,29,35}

Regarding the use of (4-fluorophenyl)hydrazine hydrochloride (7), Figure S9 and S10 show the product concentration versus experiment time and $1/[A]$ versus experiment time, respectively, for the formation of 1-(2-fluorophenyl)-3,5-dimethylpyrazole (12). Figures S11 and S12 correspond to the formation of 1-(2-fluorophenyl)-3,4,5-trimethylpyrazole (13). Figures S13 and S14 show the experimental data for the product formation of 1-(2-fluorophenyl)-5-methyl-3-phenylpyrazole (14). The reaction between (4-fluorophenyl)hydrazine hydrochloride (7) and 1-phenylbutane-1,3-dione (1) is regioselective, yielding exclusively the isomer 1-(2-fluorophenyl)-5-methyl-3-phenylpyrazole (14) as shown by the ^1H – ^{13}C HMBC correlation peak between $^1\text{H}_{\text{CH}_3}$ and the quaternary carbon 5-C, which appears at higher field than 3-C in a pyrazole ring.³⁶ In addition, an NOE interaction is observed between the methyl group and 5'-H, corroborating the presence of the methyl group in position 5 of the pyrazole ring, closer to the fluorinated ring. When using 1-phenylbutane-1,3-dione (1) with other hydrazines derivatives, the major isomer found also shows the methyl group in position 5 of the pyrazole ring.^{35,29} Three new derivatives are obtained with the use of (2,3,4,5,6-pentafluorophenyl)hydrazine hydrochloride (8) as reported above. Thus, Figures S15 and S16 show the product concentration versus experiment time and $1/[A]$ versus experiment time, respectively, for the formation of 1-(pentafluorophenyl)-3,5-dimethylpyrazole (15).³⁷ Figures S17 and S18 correspond to the formation of 1-(pentafluorophenyl)-3,4,5-trimethylpyrazole (16). Figures S19 and S20 represent the experimental data obtained for the formation of 1-(pentafluorophenyl)-5-methyl-3-phenylpyrazole (17).³² The reaction between (2,3,4,5,6-pentafluorophenyl)hydrazine hydrochloride (8) and 1-phenylbutane-1,3-dione (1) is regioselective, yielding exclusively the 1-(pentafluorophenyl)-

5-methyl-3-phenylpyrazole (17), which was checked by a ^1H – ^{13}C HMBC correlation peak between $^1\text{H}_{\text{CH}_3}$ and the quaternary carbon 5-C, which appears at higher field than 3-C in a pyrazole ring.³⁶ Owing to the unique advantages of our hyphenated system, the kinetic parameters can be obtained within a single on-flow experiment. The reaction rate constant values, the pre-exponential factor, and the activation energy are collected in Table 1, applying the same model used in previous sections.

CONCLUSIONS

The hyphenation of a nanoliter NMR microfluidic chip to a microreactor platform (Labtrix Start) enables the extraction of kinetic information, such as the rate constant, activation energy, and pre-exponential factor, within a single on-flow experiment of around 10 min. Central are the capabilities of the small-volume NMR microfluidic chip of monitoring the reaction progress before, at the onset of, and during the steady state of the reaction, combined with a fitting model. The capability of the Labtrix Start of evaluating many reaction parameters in a short period of time is dramatically improved by the hyphenation to a nanoliter NMR microfluidic chip, which not only eliminates the requirement to wait for the equilibration time, but also provides a wide variety of information related to concentration, temperature, and time that can be extracted before the Labtrix Start equilibration time is reached. Finally, the in-line NMR monitoring does not require any workup of the reaction mixture, nor is there the need to use deuterated solvents.

The efficacy of the methodology has been illustrated for the synthesis of 5-methyl-3-phenylisoxazole (3) and was extended to a library of pyrazole derivatives, extracting the kinetic information within a single nonisothermal on-flow experiment. This methodology is a rapid alternative to the time-consuming conventional isothermal methods for kinetic analysis and emphasizes the importance of flow methodologies and especially of online/in-line monitoring of chemical reactions. It can be widely used since it can be applied to most chemical processes with simultaneous or consecutive changes in reaction parameters (i.e., temperature, time) and, importantly, extended to analytical techniques other than NMR spectroscopy.

ASSOCIATED CONTENT

Supporting Information

The Supporting Information is available free of charge on the ACS Publications website at DOI: 10.1021/acs.analchem.5b02811.

Experimental data on the heating profile, Arrhenius plot of 3, reaction product concentration, and 1/reagent concentration vs time plots for the various reactions (PDF)

AUTHOR INFORMATION

Corresponding Authors

*E-mail: mariavictoria.gomez@uclm.es.

*E-mail: aldrik.velders@wur.nl.

Author Contributions

[†]M.V.G. and A.M.R. contributed equally to this work.

Notes

The authors declare no competing financial interest.

ACKNOWLEDGMENTS

We acknowledge financial support from the Spanish Ministry of Science and Innovation (Grants CTQ2011-22410 and CTQ2014-54987-P) and Junta de Comunidades de Castilla-La Mancha (Grant PEII-2014-002-A). M.V.G. thanks the Albacete Science and Technology Park for the Instituto de Recursos Humanos para la Ciencia y la Tecnología (INCRECYT) research contract and the Ministerio de Economía y Competitividad (MINECO) for participation in the Ramon y Cajal program. A.M.R. thanks the Ministry of Science and Innovation for his Formación del Profesorado Universitario (FPU) grant. A.H.V. thanks the Ministry of Education, Culture and Sport for a sabbatical stay (Grant SAB2011-0072).

REFERENCES

- (1) House, J. E. *Principles of Chemical Kinetics*; Elsevier Science: Amsterdam, 2007.
- (2) Mozharov, S.; Nordon, A.; Littlejohn, D.; Wiles, C.; Watts, P.; Dallin, P.; Girkin, J. M. *J. Am. Chem. Soc.* **2011**, *133*, 3601–3608.
- (3) Mason, B. P.; Price, K. E.; Steinbacher, J. L.; Bogdan, A. R.; McQuade, D. T. *Chem. Rev.* **2007**, *107*, 2300–2318.
- (4) Ristenpart, W. D.; Wan, J.; Stone, H. A. *Anal. Chem.* **2008**, *80*, 3270–3276.
- (5) Salmi, T.; Carucci, J. H.; Roche, M.; Eranen, K.; Warn, J.; Murzin, D. *Chem. Eng. Sci.* **2013**, *87*, 306–314.
- (6) Yue, J.; Schouten, J. C.; Nijhuis, T. A. *Ind. Eng. Chem. Res.* **2012**, *51*, 14583–14609.
- (7) McMullen, J. P.; Stone, M. T.; Buchwald, S. L.; Jensen, K. F. *Angew. Chem., Int. Ed.* **2010**, *49*, 7076–7080.
- (8) Okagbare, P. I.; Emory, J. M.; Datta, P.; Goettert, J.; Soper, S. A. *Lab Chip* **2010**, *10*, 66–73.
- (9) Prabhakar, A.; Mukherji, S. *Lab Chip* **2010**, *10*, 748–754.
- (10) Carter, C. F.; Lange, H.; Ley, S. V.; Baxendale, I. R.; Wittkamp, B.; Goode, J. G.; Gaunt, N. L. *Org. Process Res. Dev.* **2010**, *14*, 393–404.
- (11) Mozharov, S.; Nordon, A.; Girkin, J. M.; Littlejohn, D. *Lab Chip* **2010**, *10*, 2101–2107.
- (12) Polte, J.; Erler, R.; Thuenemann, A. F.; Sokolov, S.; Ahner, T. T.; Rademann, K.; Emmerling, F.; Kraehnert, R. *ACS Nano* **2010**, *4*, 1076–1082.
- (13) Wensink, H.; Benito-Lopez, F.; Hermes, D. C.; Verboom, W.; Gardeniers, H.; Reinhoudt, D. N.; van den Berg, A. *Lab Chip* **2005**, *5*, 280–284.
- (14) Dunayevskiy, Y. M.; Vouros, P.; Wintner, E. A.; Shipps, G. W.; Carell, T.; Rebek, J. *Proc. Natl. Acad. Sci. U. S. A.* **1996**, *93*, 6152–6157.
- (15) Moore, J. S.; Jensen, K. F. *Angew. Chem., Int. Ed.* **2014**, *53*, 470–473.
- (16) McMullen, J. P.; Jensen, K. F. *Org. Process Res. Dev.* **2011**, *15*, 398–407.
- (17) Ciobanu, L.; Jayawickrama, D. A.; Zhang, X. Z.; Webb, A. G.; Sweedler, J. V. *Angew. Chem., Int. Ed.* **2003**, *42*, 4669–4672.
- (18) Ernst, R. R. *Angew. Chem., Int. Ed. Engl.* **1992**, *31*, 805–823.
- (19) Sans, V.; Porwol, L.; Dragone, V.; Cronin, L. *Chem. Sci.* **2015**, *6*, 1258–1264.
- (20) Foley, D. A.; Bez, E.; Codina, A.; Colson, K. L.; Fey, M.; Krull, R.; Piroli, D.; Zell, M. T.; Marquez, B. L. *Anal. Chem.* **2014**, *86*, 12008–12013.
- (21) Fratila, R. M.; Velders, A. H. *Annu. Rev. Anal. Chem.* **2011**, *4*, 227–249.
- (22) Lacey, M. E.; Subramanian, R.; Olson, D. L.; Webb, A. G.; Sweedler, J. V. *Chem. Rev.* **1999**, *99*, 3133–3152.
- (23) Jones, C. J.; Larive, C. K. *Anal. Bioanal. Chem.* **2012**, *402*, 61–68.
- (24) Zalesskiy, S. S.; Danieli, E.; Blümich, B.; Ananikov, V. P. *Chem. Rev.* **2014**, *114*, 5641–5694.

- (25) Gomez, M. V.; Reinhoudt, D. N.; Velders, A. H. *Small* **2008**, *4*, 1293–5.
- (26) Fratila, R. M.; Gomez, M. V.; Sykora, S.; Velders, A. H. *Nat. Commun.* **2014**, *5*, 3025.
- (27) Gomez, M. V.; Verputten, H. H.; Díaz-Ortiz, A.; Moreno, A.; de la Hoz, A.; Velders, A. H. *Chem. Commun. (Cambridge, U. K.)* **2010**, *46*, 4514–6.
- (28) Rodriguez, A. M.; Juan, A.; Gomez, M. V.; Moreno, A.; De la Hoz, A. *Synthesis* **2012**, *44*, 2527–2530.
- (29) Wiles, C.; Watts, P.; Haswell, S. J.; Pombo-Villar, E. *Org. Process Res. Dev.* **2004**, *8*, 28–32.
- (30) Tang, S.; He, J.; Sun, Y.; He, L.; She, X. *Org. Lett.* **2009**, *11*, 3982–3985.
- (31) Begtrup, M.; Boyer, G.; Cabildo, P.; Cativiela, C.; Claramunt, R. M.; Elguero, J.; Garcia, J. I.; Toiron, C.; Vedso, P. *Magn. Reson. Chem.* **1993**, *31*, 107–168.
- (32) Bagrov, F. V.; Bagrov, D. F. *Zh. Org. Khim.* **1993**, *29*, 2260–2263.
- (33) Krasnoshchek, A. P.; Khmel'nitskii, R. A.; Polyakova, A. A.; Grandberg, I. I.; Minkin, V. I. *Zh. Org. Khim.* **1968**, *4*, 1690–1696.
- (34) Watts, P.; Wiles, C. *Chem. Commun.* **2007**, 443–467.
- (35) Guo, S.; Wang, J.; Guo, D.; Zhang, X.; Fan, X. *RSC Adv.* **2012**, *2*, 3772–3777.
- (36) De La Hoz, A.; Pardo, M. D. C.; Elguero, J.; Fruchier, A. *Magn. Reson. Chem.* **1989**, *27*, 603–609.
- (37) Jagerovic, N.; Elguero, J.; Aubagnac, J. L. *Tetrahedron* **1996**, *52*, 6733–6738.